New Cosmological Data and the Values of the Fundamental Parameters
IAU Symposium, Vol. 201, 2005
Anthony Lasenby and Althea Wilkinson, eds.

Cosmological Parameters from the 2dF Galaxy Redshift Survey

Matthew Colless and the 2dFGRS team[1]
Research School of Astronomy & Astrophysics
The Australian National University
Weston Creek, ACT 2611, Australia

Abstract. This paper describes the goals, current status and some preliminary results from the 2dF Galaxy Redshift Survey. In particular we present the most precise measurement to date of the redshift-space distortion parameter, $\beta \equiv \Omega^{0.6}/b = 0.39 \pm 0.05$. Combined with recent CMB anisotropy measurements, our results strongly favour a low-density universe.

1. Introduction

The main goals of the 2dF Galaxy Redshift Survey (2dFGRS) with regard to large scale structure and cosmology are:

1. To measure the galaxy power spectrum $P(k)$ on scales up to a few hundred Mpc, filling the gap between the small scales where $P(k)$ is known from previous galaxy redshift surveys and the largest scales where $P(k)$ is well-determined by observations of the cosmic microwave background (CMB) anisotropies. Particular goals are to determine the scale of the turnover in the power spectrum and to attempt to observe in the galaxy distribution the acoustic peaks already seen in the CMB power spectrum.

2. To measure the redshift-space distortion of the large-scale clustering that results from the peculiar velocity field produced by the mass distribution. This distortion depends on both the mass density parameter Ω and the bias factor b of the galaxy distribution with respect to the mass distribution, and its measurement constrains the combination $\beta \equiv \Omega^{0.6}/b$.

3. To measure higher-order clustering statistics in order to: (i) determine the bias parameter b directly, revealing the relationship between the distributions of mass and light and yielding an independent measure of Ω;

[1] *The 2dF Galaxy Redshift Survey team:* Matthew Colless (ANU), John Peacock (ROE), Carlton M. Baugh (Durham), Joss Bland-Hawthorn (AAO), Terry Bridges (AAO), Russell Cannon (AAO), Shaun Cole (Durham), Chris Collins (LJMU), Warrick Couch (UNSW), Nicholas Cross (St Andrews), Gavin Dalton (Oxford), Kathryn Deeley (UNSW), Roberto De Propris (UNSW), Simon Driver (St Andrews), George Efstathiou (IoA), Richard S. Ellis (Caltech), Carlos S. Frenk (Durham), Karl Glazebrook (JHU), Carole Jackson (ANU), Ofer Lahav (IoA), Ian Lewis (AAO), Stuart Lumsden (Leeds), Steve Maddox (Nottingham), Darren Madgwick (IoA), Peder Norberg (Durham), Will Percival (ROE), Bruce Peterson (ANU), Will Sutherland (ROE), Keith Taylor (Caltech)

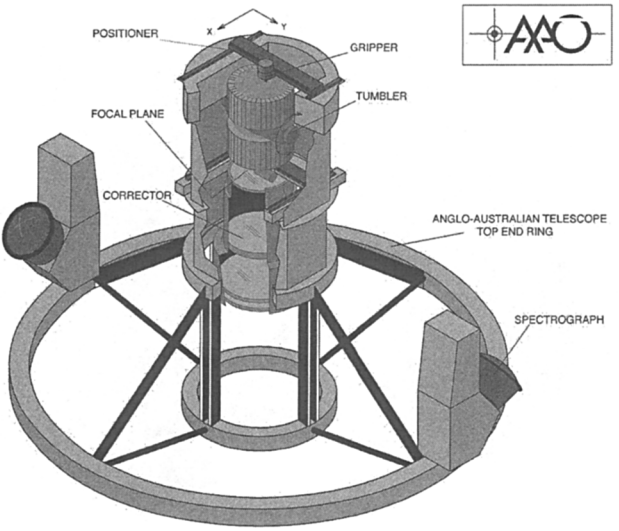

Figure 1. Schematic of the 2dF instrument.

(ii) establish whether the galaxy distribution on large scales is a Gaussian random field, as predicted by most inflationary models of the early universe; and (iii) investigate the non-linear growth of clustering in the small-scale galaxy distribution.

2. Survey Design

The survey is designed around the 2dF multi-fibre spectrograph on the Anglo-Australian Telescope, which is capable of observing up to 400 objects simultaneously over a 2 degree diameter field of view. Figure 1 shows a schematic diagram of the main components of 2dF. Full details of the instrument and its performance are given in Lewis et al. (2000).

The source catalogue for the survey is a revised and extended version of the APM galaxy catalogue (Maddox et al. 1990a,b,c). This catalogue is based on Automated Plate Measuring machine (APM) scans of 390 plates from the UK Schmidt Telescope (UKST) Southern Sky Survey. The b_J magnitude system for the Southern Sky Survey is defined by the response of Kodak IIIaJ emulsion in combination with a GG395 filter, zeropointed by CCD photometry to the Johnson B band. The extended version of the APM catalogue includes over 5 million galaxies down to b_J=20.5 in both north and south Galactic hemispheres over a region of almost 10^4 sq.deg (bounded approximately by declination $\delta \leq +3$ and Galactic latitude $b \gtrsim 20$). Figure 2 shows the galaxy distribution in the region of the catalogue around the South Galactic Pole (SGP). The photometry of the catalogue is calibrated with numerous CCD sequences and has a precision of approximately 0.2 mag for galaxies with b_J=17–19.5. The star-galaxy separation is as described in Maddox et al. (1990b), supplemented by visual validation of each galaxy image.

https://doi.org/10.1017/S0074180900216227 Published online by Cambridge University Press

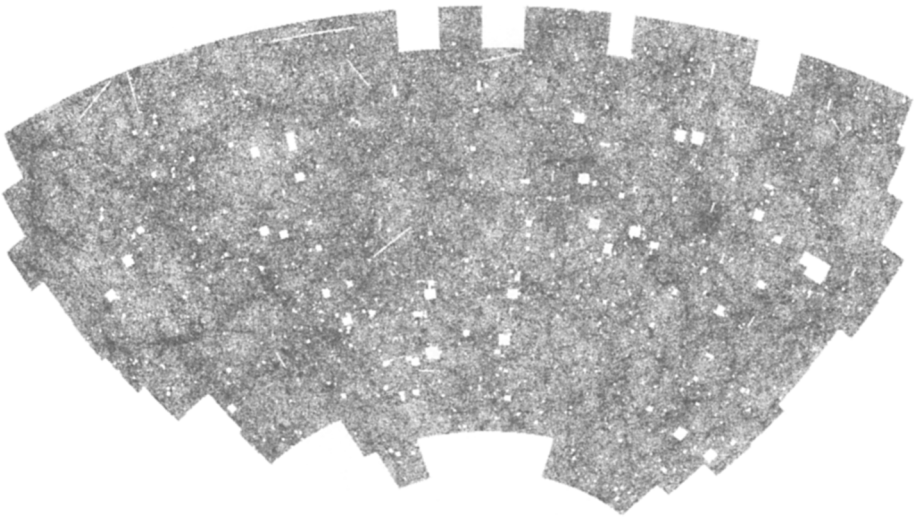

Figure 2. The galaxy distribution in the APM galaxy catalogue region around the South Galactic Pole.

The survey geometry is shown in Figure 3, and consists of two contiguous declination strips plus 100 random 2-degree fields. One strip is in the southern Galactic hemisphere and covers approximately $75^\circ \times 15^\circ$ centred close to the SGP at $(\alpha,\delta)=(01^h,-30)$; the other strip is in the northern Galactic hemisphere and covers $75^\circ \times 7.5^\circ$ centred at $(\alpha,\delta)=(12.5^h,+00)$. The 100 random fields are spread uniformly over the 7000 sq.deg region of the APM catalogue in the southern Galactic hemisphere. At the median redshift of the survey ($\bar{z}=0.11$), $100\,h^{-1}$ Mpc subtends about 20 degrees, so the two strips are $375\,h^{-1}$ Mpc long and have widths of $75\,h^{-1}$ Mpc (south) and $37.5\,h^{-1}$ Mpc (north). The volume directly sampled by the survey (out to $z=0.2$) is $3\times10^7\,h^{-3}\,\mathrm{Mpc}^3$; the volume sparsely sampled including the random fields is $1\times10^8\,h^{-3}\,\mathrm{Mpc}^3$.

The sample is limited to be brighter than an extinction-corrected magnitude of $b_J=19.45$ (using the extinction maps of Schlegel et al. 1998). This limit gives a good match between the density on the sky of galaxies and 2dF fibres. Due to clustering, however, the number in a given field varies considerably. To make efficient use of 2dF, we employ an adaptive tiling algorithm to cover the survey area with the minimum number of 2dF fields. With this algorithm we are able to achieve a 93% sampling rate with on average fewer than 5% wasted fibres per field. Over the whole area of the survey there are in excess of 250,000 galaxies.

3. Survey Status

The survey passed the half-way mark by the end of September 2000. In total, observations had been made of 148403 targets in 556 fields, yielding redshifts and identifications for 129987 galaxies, 7343 stars and 72 QSOs, at an overall completeness of 92.6%. Repeat observations have been obtained for 9583 targets.

https://doi.org/10.1017/S0074180900216227 Published online by Cambridge University Press

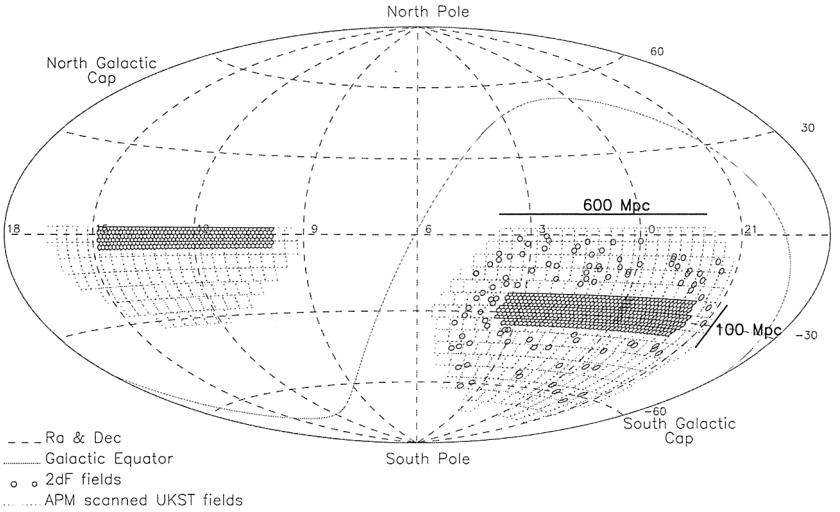

Figure 3. The 2dFGRS fields (small circles) superimposed on the APM catalogue area (dotted outlines of Sky Survey plates). There are approximately 140,000 galaxies in the $75° \times 15°$ southern strip centred on the SGP, 70,000 galaxies in the $75° \times 7.5°$ equatorial strip, and 40,000 galaxies in the 100 randomly-distributed 2dF fields covering the whole area of the APM catalogue in the south.

Figure 4 shows the projection of the galaxies in the northern and southern strips onto (α, z) slices. The main points to note are the level of detail apparent in the map and the slight variations in density with R.A. due to the varying field coverage along the strips.

Figure 5 summarises the progress of the survey so far, and the projection for the future. To the end of September 2000, the survey has had approximately 87 clear nights out of 180 allocated nights—a clear fraction of less than 50%. After a slow start, the rate of progress has levelled off at approximately 1000 new galaxy redshifts per allocated night (over 2000 per clear night). At this rate we expect to have approximately 220,000 redshifts by the time survey observations are completed at the end of 2001.

Although the adaptive tiling algorithm is efficient, and results in highly-uniform sampling when the survey is done, the sampling at this intermediate stage, with only half the fields observed, is highly variable. Figure 6 shows the completeness of the survey fields in the northern and southern strips, and illustrates the fact that a significant fraction of the fields observed to date still require observations of neighbouring tiles to achieve high completeness. The variable sampling makes quantification of the large scale structure more difficult, and limits any analysis requiring relatively uniform contiguous areas.

https://doi.org/10.1017/S0074180900216227 Published online by Cambridge University Press

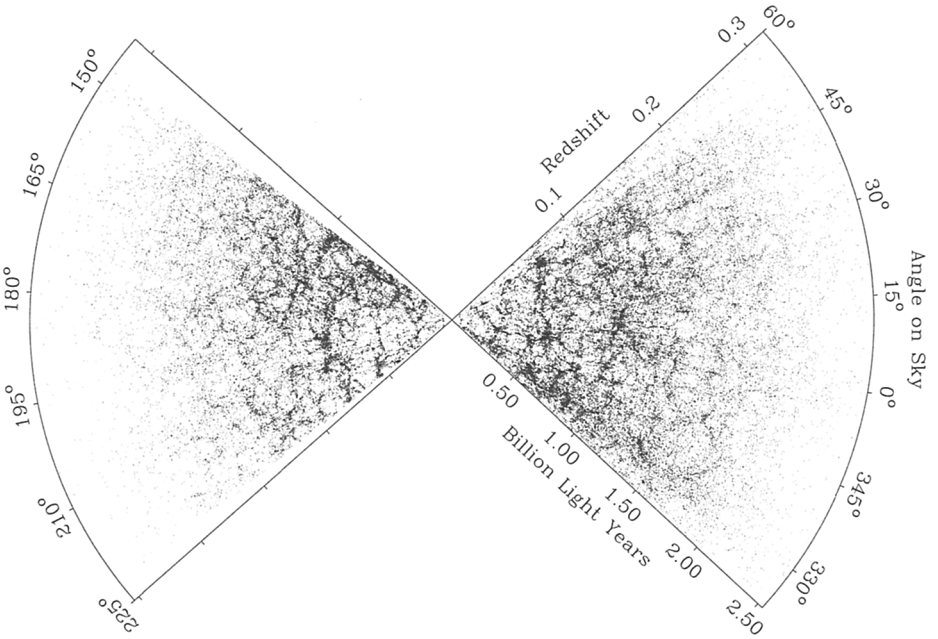

Figure 4. Projection of the galaxy distribution onto (α, z) slices.

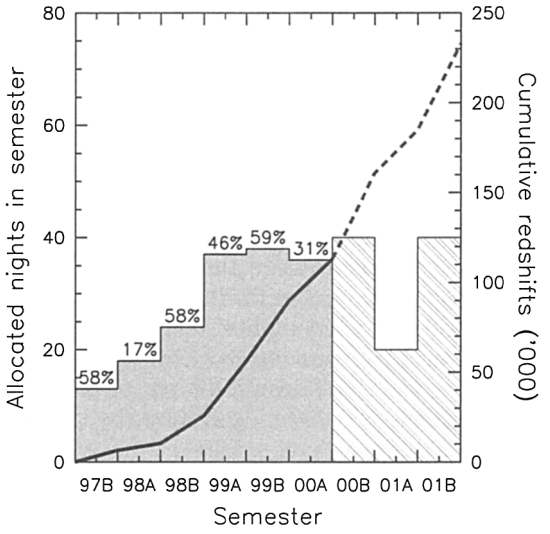

Figure 5. Progress on the 2dFGRS, showing the allocated nights per semester as the histogram and the cumulative number of redshifts as the line. The percentages are the fraction of clear nights. The predicted future progress is shown as the dashed line.

https://doi.org/10.1017/S0074180900216227 Published online by Cambridge University Press

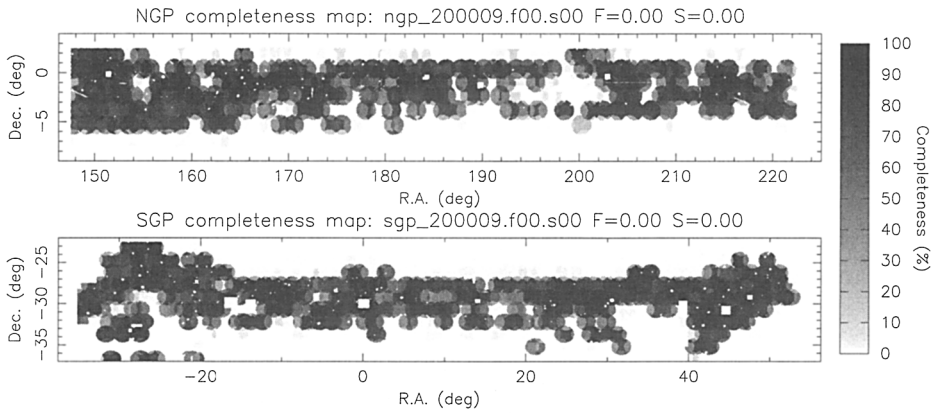

Figure 6. The completeness as a function of position on the sky. The circles are individual 2dF fields ('tiles'). Unobserved tiles result in low completeness in overlap regions. Rectangular holes are omitted regions around bright stars.

4. Large-Scale Structure and Cosmology

The simplest statistic for studying clustering in the galaxy distribution is the the two-point correlation function, $\xi(\sigma, \pi)$. This measures the excess probability over random of finding a pair of galaxies with a separation in the plane of the sky σ and a line-of-sight separation π. Because the radial separation in redshift space includes the peculiar velocity as well as the spatial separation, $\xi(\sigma, \pi)$ is anisotropic. On small scales the correlation function is extended in the radial direction due to the large peculiar velocities in non-linear structures such as groups and clusters—this is the well-known 'Figure-of-God' effect. On large scales it is compressed in the radial direction due to the coherent infall of galaxies onto mass concentrations—the Kaiser effect (Kaiser 1987).

The degree of large-scale compression of the correlation function is determined by the total mass density of the universe, Ω, and the biasing of the galaxy distribution with respect to the mass distribution. For a linear bias model, where the fractional fluctuations in the densities of galaxies and mass are linked by the proportionality constant b, the redshift-space distortion on large scales depends on the combination $\beta \equiv \Omega^{0.6}/b$. On small scales the extension of the correlation function along the line of sight is adequately approximated by allowing for the rms velocity dispersion of the galaxies in collapsed structures, σ_p.

To estimate $\xi(\sigma, \pi)$ we compare the observed count of galaxy pairs with the count estimated from a random distribution following the same selection function both on the sky (Figure 6) and in redshift (Figure 7) as the observed galaxies. We apply optimal weighting to minimise the uncertainties due to cosmic variance and Poisson noise. This is close to equal-volume weighting out to our adopted redshift limit of z=0.25. We have tested our results and found them to be robust against the uncertainties in both the survey mask and the weighting procedure.

Figure 8 shows the $\xi(\sigma, \pi)$ we obtain by this procedure. As in previous redshift surveys, the Finger-of-God effect on small scales is readily apparent.

https://doi.org/10.1017/S0074180900216227 Published online by Cambridge University Press

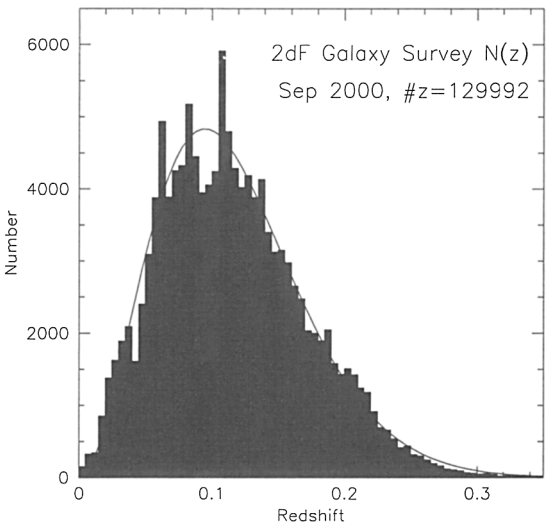

Figure 7. The redshift distribution of the 2dFGRS. The smooth curve is the prediction for a homogeneous galaxy distribution.

However the 2dFGRS is the first survey large enough to clearly show the detailed signature of the Kaiser effect in the obvious radial compression at large separations on the sky.

We quantify this compression through the quadrupole-to-monopole ratio of ξ, which in the linear regime is given by

$$\frac{\xi_2}{\xi_0} = \frac{3+n}{n} \frac{4\beta/3 + 4\beta^2/7}{1 + 2\beta/3 + \beta^2/5}$$

where n is the power spectrum index of the fluctuations, $\xi \propto r^{-(3+n)}$. This is modified by the Finger-of-God effect, which is significant even at large scales and dominant at small scales. Full details of the fitting procedure are given in Peacock et al. (2000).

Figure 9a shows the variation in ξ_2/ξ_0 as a function of scale. The ratio is positive on small scales where the Finger-of-God effect dominates, and negative on large scales where the Kaiser effect dominates. The best-fitting model (considering only the quasi-linear regime with $r{>}8\,h^{-1}\,$Mpc) has $\beta{\approx}0.4$ and $\sigma_p \approx 400\,\mathrm{km\,s^{-1}}$ (or $4\,h^{-1}\,$Mpc); the likelihood contours are shown in Figure 9b. Marginalising over σ_p, the best estimate of β and its 68% confidence interval is

$$\beta = 0.39 \pm 0.05$$

This is the first precise measurement of β from redshift-space distortions; previous studies have achieved no more than 3σ detections.

https://doi.org/10.1017/S0074180900216227 Published online by Cambridge University Press

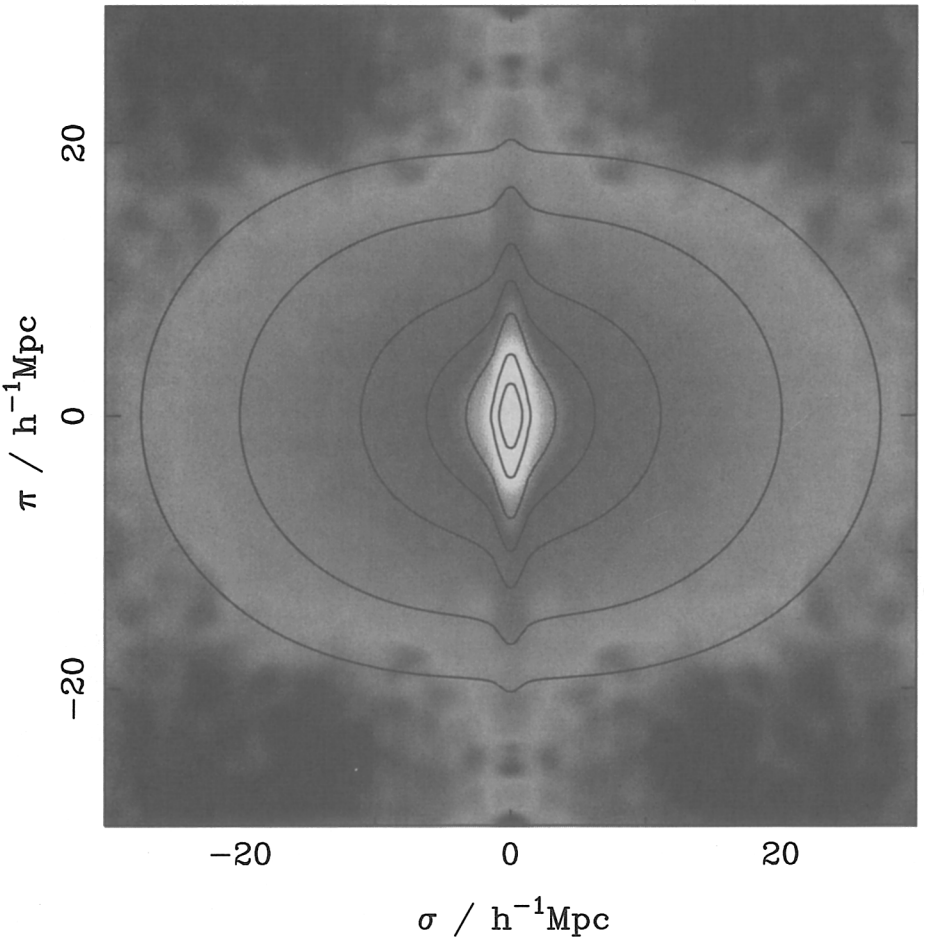

Figure 8. The galaxy correlation function $\xi(\sigma,\pi)$ as a function of transverse (σ) and radial (π) pair separation is shown as a greyscale image. It was computed in $0.2\,h^{-1}$ Mpc boxes and then smoothed with a Gaussian having an rms of $0.5\,h^{-1}$ Mpc. The contours are for a model with β=0.4 and σ_p=400 km s^{-1}, and are plotted at ξ=10, 5, 2, 1, 0.5, 0.2 and 0.1.

https://doi.org/10.1017/S0074180900216227 Published online by Cambridge University Press

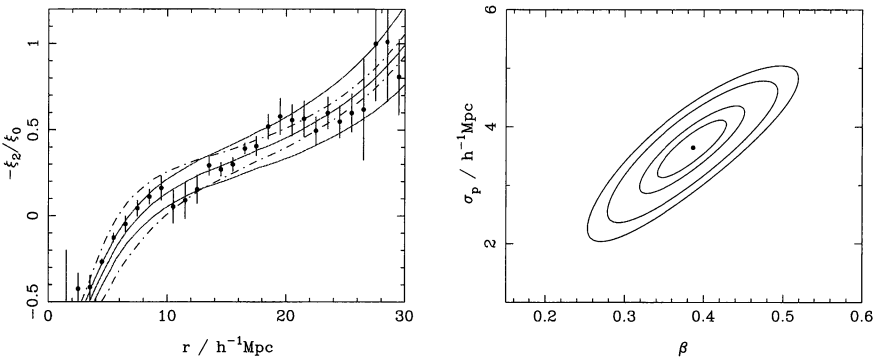

Figure 9. (a) The compression of $\xi(\sigma,\pi)$ as measured by its quadrupole-to-monopole ratio, plotted as $-\xi_2/\xi_0$. The solid lines correspond to models with σ_p=400 km s^{-1} and (bottom to top) β=0.3,0.4,0.5, while the dot-dash lines correspond to models with β=0.4 and (top to bottom) σ_p=300,400,500 km s^{-1}. (b) Likelihood contours for β and σ_p from the model fits. The inner contour is the one-parameter 68% confidence ellipse; the outer contours are the two-parameter 68%, 95% and 99% confidence ellipses. The central dot is the maximum likelihood fit, with β=0.39 and σ_p=3.7 h^{-1} Mpc.

5. Discussion

Assuming $b\approx1$, the 2dFGRS value of β naively implies a low total density, $\Omega \approx 0.21 \pm 0.04$. This is lower than, but consistent with, the total matter density estimated from recent measurements of the anisotropies in the CMB, $\Omega = 0.35 \pm 0.14$ (Jaffe et al. 2000). Corrections need to be applied to the raw 2dFGRS β to allow for the fact that the effective mean redshift of the sample is z=0.17 and the effective mean luminosity is $1.9L^*$ (Peacock et al. 2000). These corrections are uncertain, so that $\beta(z{=}0,L{=}L^*)$ could be between 5% smaller and 25% larger than $\beta(z{=}0.17,L{=}1.9L^*)$, and may reduce the difference between the 2dFGRS and CMB estimates of Ω.

The other uncertainty in converting β to Ω is the bias parameter for optical galaxies, b. Comparison of the z=0 mass power spectrum derived from the best-fit CMB model, with the galaxy power spectrum obtained by deprojecting the APM galaxy survey (Baugh & Efstathiou 1994) gives $b = 1.09 \pm 0.18$. However it will soon be possible to obtain higher-order clustering statistics from the 2dFGRS itself which will yield b directly. Simulations of the recovery of b from mock 2dFGRS surveys (Figure 10) using the redshift-space bispectrum show that it is possible to obtain ~10% precision (Verde et al. 1998).

References

Baugh, C. M. & Efstathiou, G., 1994, MNRAS, 267, 323

Jaffe, A. H., Ade, P. A. R., Balbi, A., Bock, J. J., Bond, J. R., Borrill, J., Boscaleri, A., Coble, K., Crill, B. P., de Bernardis, P., Farese, P., Ferreira, P. G., Ganga, K., Giacometti, M., Hanany, S., Hivon, E., Hristov, V. V., Iacoangeli, A., Lange, A. E., Lee, A. T., Martinis, L., Masi, S., Mauskopf, P. D., Melchiorri, A., Montroy,

https://doi.org/10.1017/S0074180900216227 Published online by Cambridge University Press

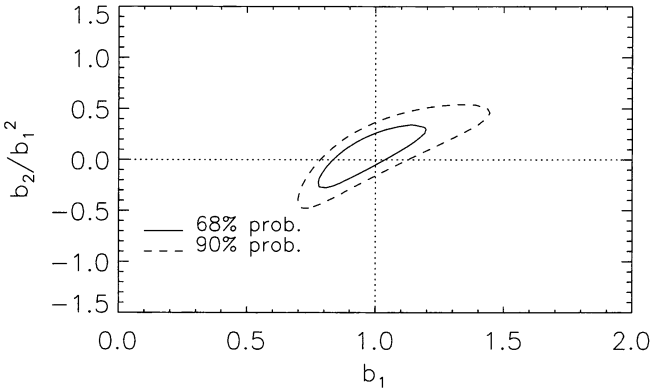

Figure 10. Recovering the bias parameters from the bispectrum.

T., Netterfield, C. B., Oh, S., Pascale, E., Piacentini, F., Pogosyan, D., Prunet, S., Rabii, B., Rao, S., Richards, P. L., Romeo, G., Ruhl, J. E., Scaramuzzi, F., Sforna, D., Smoot, G. F., Stompor, R., Winant, C. D. & Wu, J. H. P., 2000, astro-ph/0007333

Kaiser, N., 1987, MNRAS, 227, 1

Lewis, I., Taylor, K., Cannon, R. D., Glazebrook, K., Bailey, J. A., Farrell, T. J., Lankshear, A., Shortridge, K., Smith, G. A., Gray, P. M., Barton, J. R., McCowage, C., Parry, I. R., Stevenson, J., Waller, L. G., Whittard, J. D., Wilcox, J. K. & Willis, K. C., 2000, MNRAS, submitted

Maddox, S. J., Efstathiou, G., Sutherland, W. J. & Loveday, J., 1990a, MNRAS, 242, 43P

Maddox, S. J., Sutherland, W. J., Efstathiou, G. & Loveday, J., 1990b, MNRAS, 243, 692

Maddox, S. J., Efstathiou, G., Sutherland & W. J., Loveday 1990c, MNRAS, 246, 433

Peacock, J. A., Cole, S., Norberg, P., Baugh, C. M., Bland-Hawthorn, J., Bridges, T., Cannon, R. D., Colless, M. M., Collins, C. A., Couch, W. J., Dalton, G., Deeley, K. E., De Propris, R., Driver, S. P., Efstathiou, G., Ellis, R. S., Frenk, C. S., Glazebrook, K., Jackson, C. A., Lahav, O., Lewis, I. J., Lumsden, S. L., Maddox, S. J., Peterson, B. A., Price, I. A., Sutherland, W. & Taylor, K., 2000, Nature, submitted

Schlegel, D. J., Finkbeiner, D. P. & Davis, M., 1998, ApJ, 500, 525

Verde, L., Heavens, A. F., Matarrese, S. & Moscardini, L., 1998, MNRAS, 300 747